Theory of Raman scattering by surface polaritons in a four-media system



1989 J. Phys.: Condens. Matter 1 9623

(http://iopscience.iop.org/0953-8984/1/48/012)

J. Phys.: Condens. Matter **1** (1989) 9623–9636. Printed in the UK

# Theory of Raman scattering by surface polaritons in a four-media system

John S Nkoma
Physics Department, University of Botswana, Private Bag 0022, Gaborone, Botswana

Received 1 September 1988, in final form 6 March 1989

**Abstract.** The method of linear reponse theory is used to determine the response functions for surface polaritons in a four-media system (or bounded bilayer). The dispersion relation is found when the pole of the derived response function vanishes. The expressions for the scattered intensity for both back and forward scattering are derived. The scattered intensity depends on a polarisation which is the result of the coupling of the incident light to the vibrational coordinates and electric fields associated with electric-dipole-active lattice vibrations in the bilayer. Expressions for the Raman cross section by surface polaritons in the four-media system are derived for both back and forward scattering. Numerical results are presented by using parameters for a sapphire substrate–GaP–GaAs bilayer–vacuum system.

## 1. Introduction

There has been considerable interest in the properties of *surface* polaritons (SPs) in *semi-infinite* media and *thin* films (Ushioda 1981, Ushioda and Loudon 1982, Mirlin 1982, Boardman 1982, Cottam and Maradudin 1984), in addition to the study of polaritons in *bulk* (see the reviews by Barker and Loudon (1972) and Mills and Burstein (1974)). Recently, attention has turned to the properties of SPs in *superlattices* (see, e.g., Camley and Mills 1984, Szenics *et al* 1986, Nkoma 1987a, b, c). Superlattices are artificially fabricated crystals of alternate layers of two materials produced, for example, by molecular beam epitaxy. The basic unit of binary superlattices is the bilayer, and it is important to understand the properties of this system when it is bounded by two other media, hence constituting a *four-media system* (FMS), to which this paper will be devoted. The study of properties of SPs in a FMS has been pursued by a few researchers, such as by Wendler (1984, 1985) and Wendler and Haupt (1986), and they also studied guided wave polaritons supported by this system.

The main *experimental* techniques for investigating SPs have been attenuated total reflection (ATR) first proposed by Otto (1968) and Raman spectroscopy (see, e.g., Prieur and Ushioda 1975, Ushioda 1981). The theory for ATR experiments in various configurations, including the Kretschmann–Raether configuration, has been reported in several papers, e.g. for a FMS by Wendler and Haupt (1987) and for superlattices by Raj *et al* (1987) and Haupt and Wendler (1987). On the other hand, theories of Raman scattering have mainly been by two equivalent approaches, namely the linear response theory (Barker and Loudon 1972) and a Green function formalism (Maradudin and

0953-8984/89/489623 + 14 $02.50  

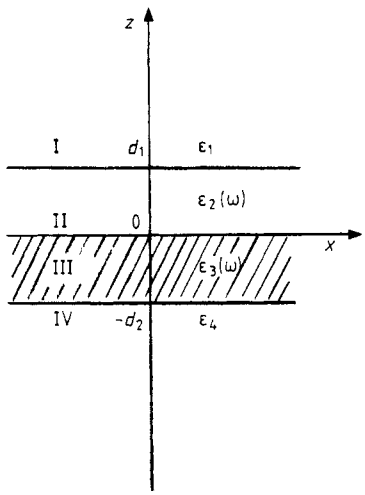


**Figure 1.** The geometry of a FMS modelling a sapphire substrate–GaP–GaAs bilayer–vacuum with dielectric functions $\varepsilon_4$, $\varepsilon_3(\omega)$, $\varepsilon_2(\omega)$ and $\varepsilon_1$, respectively.

Mills 1975). The linear response theory has been used to find the Raman scattering cross section by SPS in a semi-infinite media (Nkoma and Loudon 1975), in a thin film (Nkoma 1975) and in binary superlattices (Babiker *et al* 1987a, b), while the Green function formalism has been used to study Raman scattering by SPS in a semi-infinite media and thin films (Chen *et al* 1975, Mills *et al* 1976). To our knowledge, the theory of Raman scattering by SPS in a FMS has not as yet been reported and, in view of the importance of this geometry towards understanding binary superlattice structures, this paper will be devoted to developing such a theory, using the linear response formalism.

The organisation of this paper is as follows. In § 2, we describe the response of the SP electric fields to an externally applied polarisation and derive the SP response functions. The poles of the derived response functions give the dispersion relation for SPS in the FMS. Section 3 is devoted to an analysis of the light scattering by SPS in the FMS. The relevant expressions for the scattered intensity are derived for both back and forward scattering. The scattered intensities are found to be related to the polarisation which is formed by the coupling of the incident light to the vibrational coordinates and electric fields associated with the electric-dipole-active lattice vibrations in the bilayer. The Raman scattering cross section will be shown to depend on the electric field fluctuations, which can be evaluated using the fluctuation–dissipation theorem (Landau and Lifshitz 1969) in conjunction with the reponse functions derived in § 2. Numerical results and discussion are presented in § 4 where the FMS is modelled by parameters for a sapphire–GaP–GaAs bilayer–vacuum system. Finally, concluding remarks are made in § 5.

## 2. Linear response theory and the dispersion relation for SPS in a FMS

A schematic representation of the FMS that we are considering is shown in figure 1, consisting of region I ($z > d_1$) with a positive dielectric constant $\varepsilon_1$, region II ($0 < z < d_1$) which has a frequency-dependent dielectric function $\varepsilon_2(\omega)$, region III ($-d_2 < z < 0$) which has another frequency-dependent dielectric function $\varepsilon_3(\omega)$, and region IV ($z < -d_2$) which has a positive dielectric constant $\varepsilon_4$. Thus, the bilayer consisting of

regions II and II is of thickness $d_1 + d_2$. Consider the response of SPS in this geometry to some externally applied polarisation

$$\boldsymbol{P} = \boldsymbol{P}^{\text{ext}} \exp[\mathrm{i}(\boldsymbol{Q} \cdot \boldsymbol{r} - \omega t)]. \tag{1}$$

We apply the linear response theory (see details, for example, in the papers by Nkoma and Loudon (1975) and Nkoma (1975)) to obtain the response functions. After a long somewhat tedious enumeration and rearrangement of terms, one obtains the response to the external polarisation $\boldsymbol{p}^{\text{ext}}$ in the following form:

$$\boldsymbol{E}_{2i} = \langle\!\langle E_i ; E_j \rangle\!\rangle_{\text{tot}} \boldsymbol{P}_j^{\text{ext}} \tag{2}$$

where

$$\langle\!\langle E_i ; E_j \rangle\!\rangle_{\text{tot}} = \langle\!\langle E_i ; E_j \rangle\!\rangle_{\text{B}} + \langle\!\langle E_i , E_j \rangle\!\rangle_{\text{S}} \tag{3}$$

where the first term describes the bulk response and the second term describes the surface response. We shall concentrate our attention on the surface response only, and this is given by

$$\begin{aligned}
\langle\!\langle E_i ; E_j \rangle\!\rangle_{\text{S}} = {} & [\exp(\mathrm{i}q_{2z}z)/\varepsilon_0\Delta]\,[\![\rho_1\{\exp(\mathrm{i}q_{3z}d_2)\,[R^{+}_{ij12} + \exp(-\mathrm{i}q_{2z}d_1)\,\alpha_{ij}R^{+}_{ij23}] \\
& + 2\varepsilon_2(\omega)\gamma_{ij}\exp(-\mathrm{i}q_{2z}d_1)\,R^{+}_{ij23}R^{+}_{ij34}\} \\
& + \rho_2\{\exp(-\mathrm{i}q_{3z}d_2)\,[R^{+}_{ij12} + \exp(-\mathrm{i}q_{2z}d_1)\,\alpha_{ij}R^{-}_{ij23}]\}]\!] \\
& + [\exp(-\mathrm{i}q_{2z}z)/\varepsilon_0\Delta]\,\theta_{ij}\,[\![\rho_3\{\exp(\mathrm{i}q_{3z}d_2)\,[R^{-}_{ij12} + \exp(\mathrm{i}q_{2z}d_1)\,\alpha_{ij}R^{-}_{ij23}] \\
& + 2\varepsilon_2(\omega)\gamma_{ij}\exp(\mathrm{i}q_{2z}d_1)\,R^{-}_{ij23}R^{-}_{ij34}\} \\
& + \rho_4\{\exp(-\mathrm{i}q_{3z}d_2)\,[R^{-}_{ij12} + \exp(\mathrm{i}q_{2z}d_1)\,\alpha_{ij}R^{+}_{ij23}]\}]\!]
\end{aligned} \tag{4}$$

where

$$\rho_1 = [\varepsilon_4 q_{3z} + \varepsilon_3(\omega)q_{4z}][\varepsilon_3(\omega)q_{2z} + \varepsilon_2(\omega)q_{3z}][\varepsilon_2(\omega)q_{1z} + \varepsilon_1 q_{2z}] \tag{5}$$

$$\rho_2 = [\varepsilon_4 q_{3z} - \varepsilon_3(\omega)q_{4z}][\varepsilon_3(\omega)q_{2z} - \varepsilon_2(\omega)q_{3z}]\,[\varepsilon_2(\omega)q_{1z} + \varepsilon_1 q_{2z}] \tag{6}$$

$$\rho_3 = [\varepsilon_4 q_{3z} + \varepsilon_3(\omega)q_{4z}][\varepsilon_3(\omega)q_{2z} - \varepsilon_2(\omega)q_{3z}][\varepsilon_1 q_{2z} - \varepsilon_2(\omega)q_{1z}] \tag{7}$$

$$\rho_4 = [\varepsilon_4 q_{3z} - \varepsilon_3(\omega)q_{4z}][\varepsilon_3(\omega)q_{2z} + \varepsilon_2(\omega)q_{3z}][\varepsilon_1 q_{2z} - \varepsilon_2(\omega)q_{1z}] \tag{8}$$

and $\alpha_{ij}$, $\gamma_{ij}$ and $\theta_{ij}$ are given by

$$\alpha_{xx} = \alpha_{zx} = 1 - \varepsilon_2(\omega)/\varepsilon_3(\omega) \tag{9}$$

$$\alpha_{xz} = \alpha_{zz} = q_2^2/q_{2z}^2 - q_3^2/q_{3z}^2 \tag{10}$$

$$\gamma_{xx} = \gamma_{xz} = 1 \tag{11}$$

$$\gamma_{zx} = \gamma_{zz} = q_{3z}/q_{2z} \tag{12}$$

$$\theta_{xx} = \theta_{xz} = 1 \tag{13}$$

$$\theta_{zx} = \theta_{zz} = -1 \tag{14}$$

and the resonant denominator $\Delta$ is given by

$$\begin{aligned}
\Delta = {} & \exp(\mathrm{i}q_{3z}d_2)\exp(\mathrm{i}q_{2z}d_1)\,[\rho_1 + \rho_2\exp(-2\mathrm{i}q_{3z}d_2)] \\
& \times [\varepsilon_1 q_{2z} - \varepsilon_2(\omega)q_{1z}]/[\varepsilon_1 q_{2z} + \varepsilon_2(\omega)q_{1z}]
\end{aligned}$$

$$- \exp(iq_{3z}d_2)\exp(iq_{2z}d_1)[\rho_3 + \rho_4 \exp(-2iq_{3z}d_2)]$$
$$\times [\varepsilon_1 q_{2z} + \varepsilon_2(\omega)q_{1z}]/[\varepsilon_1 q_{2z} - \varepsilon_2(\omega)q_{1z}] \tag{15}$$

where $\rho_1$, $\rho_2$, $\rho_3$, $\rho_4$ have been defined earlier in equations (5)–(8). In equation (4), $R^{\pm}_{ij12}$, $R^{\pm}_{ij23}$ and $R^{\pm}_{ij34}$ are matrix elements of $2 \times 2$ matrices $\mathbf{R}^{\pm}_{12}$, $\mathbf{R}^{\pm}_{23}$ and $\boldsymbol{R}^{\pm}_{34}$, respectively. These can be recognised to be terms corresponding to the various interfaces between regions I, II, III and IV. This feature was also observed in the linear response theory for a thin film (Nkoma 1975) and in fact, as a useful check to these results, when regions II and III are occupied by the same material, equation (4) reduces to the analogous equation for the thin film in the reference just quoted above. The matrices are given below where the superscripts $^{\pm}$ refer to upper and lower signs in all the equations.

$$\boldsymbol{R}^{\pm}_{12} = \begin{bmatrix} \pm(q_1^2 q_{2z}/q_2^2)/D^{\pm}_{12} & \pm(q_2^2 q_{1z}/q_{2z}Q_x)/D^{\pm}_{12} \\ \mp(q_1^2 Q_x/q_2^2)/D^{\pm}_{12} & \mp(q_2^2 q_{1z}/q_{2z}^2)/D^{\pm}_{12} \end{bmatrix}$$

where

$$D^{\pm}_{12} = \varepsilon_1 q_{2z} \pm \varepsilon_2(\omega)q_{1z} \tag{16}$$

and

$$\mathbf{R}^{\pm}_{23} = \begin{bmatrix} \mp(q_3^2 q_{2z}/q_2^2)/D^{\pm}_{23} & \mp(q_3^2 q_{2z}/q_{3z}Q_x)/D^{\pm}_{23} \\ \pm(q_3^2 Q_x/q_2^2)/D^{\pm}_{23} & \pm(q_3^2/q_{3z})/D^{\pm}_{23} \end{bmatrix}$$

where

$$D^{\pm}_{23} = \varepsilon_3(\omega)q_{2z} \pm \varepsilon_2(\omega)q_{3z} \tag{17}$$

and

$$\mathbf{R}^{\pm}_{34} = \begin{bmatrix} \pm(q_4^2 q_{3z}/q_3^2)/D^{\pm}_{34} & \pm(q_3^2 q_{4z}/q_{3z}Q_x)/D^{\pm}_{34} \\ \mp(q_4^2 Q_x/q_3^2)/D^{\pm}_{34} & \mp(q_3^2 q_{4z}/q_{3z}^2)/D^{\pm}_{34} \end{bmatrix}$$

where

$$D^{\pm}_{34} = \varepsilon_4 q_{3z} \pm \varepsilon_3(\omega)q_{4z}. \tag{18}$$

The dispersion relation is generated when the pole of the response function vanishes, i.e. when

$$\Delta = 0 \tag{19}$$

where $\Delta$ is given by equation (15). SPS exist in the frequency range for which the dielectric functions $\varepsilon_\beta(\omega)$ are negative and real, and hence the normal components of the wavevectors are purely imaginary according to

$$q_{1z} \rightarrow i\alpha_1 \qquad q_{2z} \rightarrow i\alpha_2 \qquad q_{3z} \rightarrow -i\alpha_3 \qquad q_{4z} \rightarrow -i\alpha_4 \tag{20}$$

such that all the SP fields decay away exponentially and equation (15) together with (19) give

$$\varepsilon_2(\omega)\varepsilon_3(\omega)\alpha_2\alpha_3(\varepsilon_4\alpha_1 + \varepsilon_1\alpha_4)$$
$$+ \varepsilon_3(\omega)\alpha_3[\varepsilon_1\varepsilon_4\alpha_2^2 + \varepsilon_2^2(\omega)\alpha_1\alpha_4]\tanh(\alpha_2 d_1)$$
$$+ \varepsilon_2(\omega)\alpha_2[\varepsilon_1\varepsilon_4\alpha_3^2 + \varepsilon_3^2(\omega)\alpha_1\alpha_4]\tanh(\alpha_3 d_2)$$

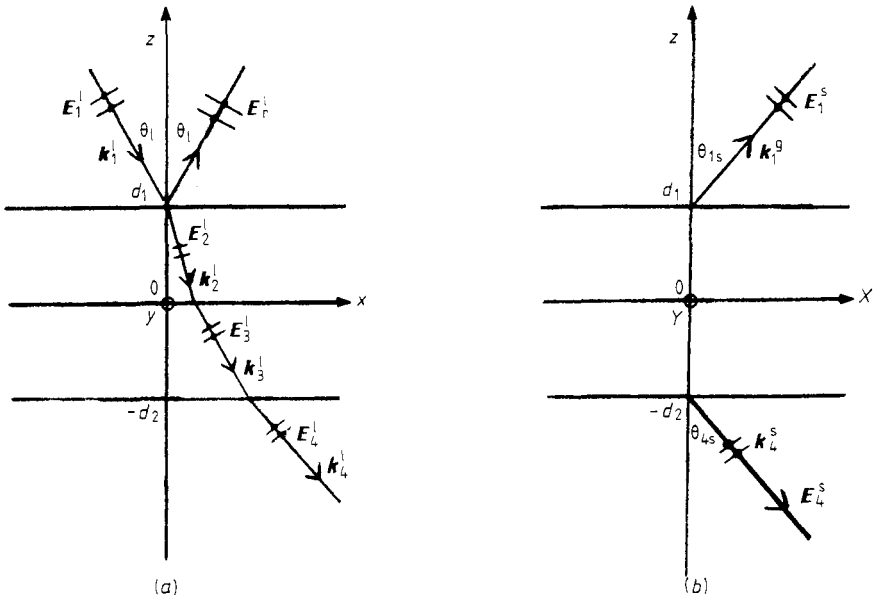


**Figure 2.** (*a*) The incidence plane *xyz* showing the incident field $E_1^{\downarrow}$ and transmitted fields $E_2^{\downarrow}$, and $E_3^{\downarrow}$ and the emerging field $E_4^{\downarrow}$ with their wavevectors, and the angle of incidence $\theta_1$. Multiple reflections in the layers have not been shown. (*b*) The scattering plane *XYz* showing the back-scattered field $E_1^{s}$ and forward-scattered field $E_4^{s}$ with their wavevectors, and respective scattering angles $\theta_{1s}$ and $\theta_{4s}$.

$$+ [\varepsilon_4 \varepsilon_2^2(\omega)\alpha_1 \alpha_3^2 + \varepsilon_1^2 \varepsilon_3(\omega)\alpha_4 \alpha_2^2] \tanh(\alpha_2 d_1) \tanh(\alpha_3 d_2) = 0. \qquad (21)$$

The response functions given in equation (4) and the dispersion relation obtained as equation (21) are the main results of this section. It should be mentioned that the dispersion equation in (21) generalises the result given by Wendler and Haupt (1986) who considered a geometry where $\varepsilon_1 = \varepsilon_4 = 1.0$ and $\alpha_1 = \alpha_4 = \alpha_0$. The dispersion curves are plotted in § 4.

## 3. Light scattering by SPS in a FMS

### *3.1. The scattering process*

In this section, we discuss the scattering of light by SPS in a FMS. The scattering process can be broken into *three* stages. In the *first stage*, illustrated in figure 2(*a*), light with an electric field $E_1^{\downarrow}$ and wavevector $k_1^{\downarrow}$, frequency $\omega_1$ is incident at the boundary $z = d_1$, where it is reflected as $E_r^{\uparrow}$ and transmitted into the bilayer where it becomes $E_2^{\downarrow}$ and $E_3^{\downarrow}$ in regions II and III, respectively, where there will be multiple reflections, and finally some light emerges in region IV with an electric field $E_4^{\downarrow}$ of wavevector $k_4^{\downarrow}$. In the *second stage*, there is interaction between the transmitted fields $E_2^{\downarrow}$ and $E_3^{\downarrow}$ and the SPS in regions II and III, respectively. In general, this interaction is complex, and the fundamental processes that finally give rise to back and forward scattering have been illustrated diagrammatically by Mills *et al* (1976) for the thin-film case. However, the result of this

interaction is to create an oscillating polarisation in the two regions of the bilayer, of the form

$$P_{\beta}^{s} \exp[i(\boldsymbol{K}_{\beta} \cdot \boldsymbol{r} - \omega_s t)] \tag{22}$$

where

$$\omega_s = \omega_1 - \omega \tag{23}$$

$$K_{\beta}^2 = K_{\beta x}^2 + K_{\beta z}^2 \tag{24}$$

$$K_{\beta x} = k_{\beta x}^1 - q_{2x} \tag{25}$$

$$K_{\beta z} = k_{\beta \xi}^1 \pm q_{\beta z}. \tag{26}$$

In the preceding equations, $\omega_s$ is the scattered frequency, and the $\pm q_{\beta z}$ combination in equation (26) arises because the SP amplitude decays from two boundaries in both regions of the bilayer. In the *third stage*, which is final, the oscillating polarisation produces the back-scattered field $\boldsymbol{E}_1^s$ and forward-scattered field $\boldsymbol{E}_4^s$ as illustrated in figure 2(*b*). Generally, the scattering plane *XYz* need not coincide with the incidence plane *xyz*. The wavevectors for the scattered fields are given by

$$k_{\alpha}^s = (\omega_s/c)\varepsilon_{\alpha}^{1/2} \tag{27}$$

$$k_{\beta}^s = (\omega_s/c)\varepsilon_{\beta}^{1/2}(\omega_s) \tag{28}$$

and, again, parallel components are conserved; together with (25), we have

$$k_{\alpha x}^s = k_{\beta x}^s = K_{\beta x} = (\omega_s/c)\varepsilon_{\alpha}^{1/2} \sin\theta_{\alpha s} (= K_x \text{ say}) \tag{29}$$

where $\varepsilon_{\alpha} = \varepsilon_1$ or $\varepsilon_4$, and $\theta_{\alpha s} = \theta_{1s}$ or $\theta_{4s}$ for back or forward scattering, respectively. The normal components are given by

$$k_{iz}^s = (\omega_s/c)(\varepsilon_i - \varepsilon_{\alpha} \sin^2\theta_{\alpha s})^{1/2} \tag{30}$$

where $i = 1, 2, 3, 4$ and noting that $\varepsilon_2 = \varepsilon_2(\omega_s)$, $\varepsilon_3 = \varepsilon_3(\omega_s)$. The scattered fields $\boldsymbol{E}_1^s$ for back scattering and $\boldsymbol{E}_4^s$ for forward scattering are obtained by solving Maxwell's equations in the four regions, with the polarisation (22) in the bilayer portion of the FMS. The calculations are long and we present the results with some comments. These calculations show that $\boldsymbol{E}_1^s$ and $\boldsymbol{E}_4^s$ have terms describing scattering by *both* bulk and surface polaritons. The terms describing scattering by bulk polaritons appear with the factor

$$\{\varepsilon_{\beta}(\omega_s)[K_{\beta}^2 - \varepsilon_{\beta}(\omega_s)\omega_s^2/c^2]\}^{-1} \tag{31}$$

which can immediately be recognised to describe scattering by LO phonons and TO phonons. Such terms are neglected since in this paper we are only interested in scattering by SPS. In doing this, we noted that all terms which describe scattering by surface excitations have the factor

$$(K_{\beta z} \pm k_{\beta z}^s)^{-1} \tag{32}$$

in agreement with previous treatments of scattering by surface excitations (Mills *et al* 1970, 1976, Chen *et al* 1975, Nkoma and London 1975). This means that, for formulations of several layers as here or in superlattices, factors such as given in equation (32) should

appear for each layer. Bearing in mind the points raised concerning equations (31) and (32), we obtain the back-scattered electric field components as follows:

$$\begin{aligned}E^{s}_{1f} = {} & (\omega_s/\varepsilon_0 c\Delta_f)\exp(\mathrm{i}\boldsymbol{k}^{s}_{1}\cdot\boldsymbol{r})\exp(-\mathrm{i}k^{s}_{1z}d_1)\\ & \times([[\exp(\mathrm{i}k^{s}_{3z}d_2)/(K_{2z}+k^{s}_{2z})]\{\varphi_{1f}g^{+}_{fh12}\exp[\mathrm{i}(K_{2z}+k^{s}_{2z})d_1]\,\eta_{fh}\\ & +\varphi_{3f}g^{-}_{fh12}\exp[\mathrm{i}(K_{2z}-k^{s}_{2z})d_1]-\varphi_{1f}g^{+}_{fh23}\zeta_{fh}-\varphi_{3f}g^{-}_{fh23}\zeta_{fh}\}\\ & +[\exp(-\mathrm{i}k^{s}_{3z}d_2)/(K_{2z}-k^{s}_{2z})]\{\varphi_{2f}g^{+}_{h12}\exp[\mathrm{i}(K_{2z}+k^{s}_{2z}d_1)]\,\eta_{fh}\\ & +\varphi_{4f}g^{-}_{fh12}\exp[\mathrm{i}(K_{2z}-k^{s}_{2z})d_1]\,\eta_{fh}-\varphi_{2f}g^{-}_{fh23}\zeta_{fh}-\varphi_{4f}g^{+}_{fh23}\zeta_{fh}\}]]P^{s}_{2h}\\ & +\{[\exp(\mathrm{i}k^{s}_{3z}d_2)/(K_{3z}+k^{s}_{3z})][(\varphi_{1f}g^{+}_{fh23}+\varphi_{3f}g^{-}_{fh23})\\ & +[2\varepsilon_3(\omega_s)/k^{s}_{3z}]\exp[-\mathrm{i}(K_{3z}+k^{s}_{3z})d_2)\,g^{+}_{fh34}(\varphi_{3f}g^{-}_{fh23}+\varphi_{1f}g^{+}_{fh23})]\\ & +[\exp(-\mathrm{i}k^{s}_{3z}d_2)/(K_{3z}-k^{s}_{3z})](\varphi_{2f}g^{-}_{fh23}+\varphi_{4f}g^{+}_{fh23})\}P^{s}_{3h}) \qquad (33)\end{aligned}$$

where a repeated subscript on the right-hand side implies summation in equation (33) and subsequent equations. Also, for $f = x, z$, the various quantities are given as

$$\varphi_{1f} = [\varepsilon_4 k^{s}_{3z}+\varepsilon_3(\omega_s)k^{s}_{4z}][\varepsilon_3(\omega_s)k^{s}_{2z}+\varepsilon_2(\omega_s)k^{s}_{3z}][\varepsilon_1 k^{s}_{2z}+\varepsilon_2(\omega_s)k^{s}_{1z}] \qquad (34)$$

$$\varphi_{2f} = [\varepsilon_4 k^{s}_{3z}+\varepsilon_3(\omega_s)k^{s}_{4z}][\varepsilon_3(\omega_s)k^{s}_{2z}-\varepsilon_2(\omega_s)k^{s}_{3z}][\varepsilon_1 k^{s}_{2z}+\varepsilon_2(\omega_s)k^{s}_{1z}] \qquad (35)$$

$$\varphi_{3f} = [\varepsilon_4 k^{s}_{3z}+\varepsilon_3(\omega_s)k^{s}_{4z}][\varepsilon_3(\omega_s)k^{s}_{2z}-\varepsilon_2(\omega_s)k^{s}_{3z}][\varepsilon_1 k^{s}_{2z}-\varepsilon_2(\omega_s)k^{s}_{1z}] \qquad (36)$$

$$\varphi_{4f} = [\varepsilon_4 k^{s}_{3z}-\varepsilon_3(\omega_s)k^{s}_{4z}][\varepsilon_3(\omega_s)k^{s}_{2z}+\varepsilon_2(\omega_s)k^{s}_{3z}][\varepsilon_1 k^{s}_{2z}-\varepsilon_2(\omega_s)k^{s}_{1z}] \qquad (37)$$

and $g^{\pm}_{fh12}$, $g^{\pm}_{fh23}$ and $g^{\pm}_{fh34}$ in (33) are matrix elements of the form discussed by Mills *et al* (1970), Nkoma and Loudon (1975) and Nkoma (1975). Also, we have $\eta_{fh}$ and $\eta_{fh}$ such that

$$\eta_{xx} = \eta_{zx} = 1 \qquad (38)$$

$$\eta_{xz} = \eta_{zz} = \varepsilon_1/\varepsilon_2(\omega_s) \qquad (39)$$

$$\zeta_{xx} = \zeta_{zx} = 1 \qquad (40)$$

$$\zeta_{xz} = \zeta_{zz} = \varepsilon_3(\omega_s)/\varepsilon_2(\omega_s) \qquad (41)$$

and the denominator $\Delta_f$ for the scattered light is given by

$$\begin{aligned}\Delta_f = {} & \exp(\mathrm{i}k^{s}_{3z}d_2)\exp(\mathrm{i}k^{s}_{2z}d_1)[\varphi_{1f}+\varphi_{2f}\exp(-\mathrm{i}2k^{s}_{3z}d_2)]\\ & \times[\varepsilon_1 k^{s}_{2z}-\varepsilon_2(\omega_s)k^{s}_{1z}]/[\varepsilon_1 k^{s}_{2z}+\varepsilon_2(\omega_s)k^{s}_{1z}]\\ & -\exp(\mathrm{i}k^{s}_{3z}d_2)\exp(-\mathrm{i}k^{s}_{2z}d_1)\,[\varphi_{3f}+\varphi_{4f}\exp(-\mathrm{i}2k^{s}_{3z}d_2)]\\ & \times[\varepsilon_1 k^{s}_{2z}+\varepsilon_2(\omega_s)k^{s}_{1z}]/[\varepsilon_1 k^{s}_{2z}-\varepsilon_2(\omega_s)k^{s}_{1z}]. \qquad (42)\end{aligned}$$

When $f = y$, equations (34)–(42) take a similar form, but with all $\varepsilon_i \to 1$ ($i = 1, 2, 3, 4$). This is a common feature for the $y$-polarisation (see, e.g. Mills *et al* 1970, Nkoma 1975). The forward-scattered electric field components are given by

$$\begin{aligned}E^{s}_{4f} = {} & (\omega_s/\varepsilon_0 c\Delta_f)\exp(\mathrm{i}\boldsymbol{k}^{s}_{4}\cdot\boldsymbol{r})\exp(\mathrm{i}k^{s}_{4z}d_2)\\ & \times([[\exp(\mathrm{i}k^{s}_{2z}d_1)/(K_{2z}-k^{s}_{2z})]\{(\varphi_{3f}g^{-}_{fh23}+\varphi_{4f}g^{+}_{fh23})\\ & +[2\varepsilon_2(\omega_s)/k^{s}_{2z}]\exp[\mathrm{i}(K_{2z}-k^{s}_{2z})d_1]\,g^{-}_{fh12}(\varphi_{3f}g^{-}_{fh23}+\varphi_{4f}g^{+}_{fh23})\}\end{aligned}$$

$$+ [\exp(-ik^{s}_{2x}d_1)/(K_{2z} + k^{s}_{2z})](\varphi_{1f}g^{+}_{fh23} + \varphi_{2f}g^{-}_{fh23})]P^{s}_{2h}$$
$$+ [[\exp(ik^{s}_{2z}d_1)/(K_{3z} - k^{s}_{3z})]\{\varphi_{3f}g^{+}_{fh34}\exp[-i(K_{3z} + k^{s}_{3z})d_2]$$
$$+ \varphi_{4f}g^{-}_{fh34}\exp[-i(K_{3z} - k^{s}_{3z})d_2] - \varphi_{3f}g^{-}_{fh23} - \varphi_{4f}g^{+}_{fh23}\}$$
$$+ [\exp(-ik^{s}_{2z}d_1)/(K_{3z} + k^{s}_{3z})]\{\varphi_{1f}g^{+}_{fh34}\exp[-i(K_{3z} + k^{s}_{3z})d_2]$$
$$+ \varphi_{2f}g^{-}_{fh34}\exp[-i(K_{3z} - k^{s}_{3z})d_2] - \varphi_{1f}g^{+}_{fh23} - \varphi_{2f}g^{-}_{fh23}\}]P^{s}_{3h}) \tag{43}$$

where all symbols are as defined earlier. It is useful to consider the limit when regions III and IV are the same, i.e. the thin-film limit, when it can be seen that $\varphi_{2f} \to 0$, $\varphi_{4f} \to 0$ and $P^{s}_{3h}$, and the back-scattered field (33) will only be dependent on the terms with the factor

$$(K_{2z} + k^{s}_{2z})^{-1} \tag{44}$$

and this term is very small because the denominator is very large, of the order of $10^6\ \mathrm{cm}^{-1}$, thus making back scattering in thin films rather weak. The forward-scattered fields given in (43) will also have terms with the factor

$$(K_{2z} - k^{s}_{2z})^{-1} \tag{45}$$

which is large because the denominator is small, and hence the forward scattering through thin films is large (Chen *et al* 1975, Prieur and Ushioda 1975, Nkoma 1975, Mills *et al* 1976). However, such conclusions for the FMS that we are studying in this paper need more care. In the present geometry, even if terms with the factor (44) are neglected in the scattered fields given in (33) and (43), there still remain terms with the factor (45). Further, the thicknesses $d_1$ and $d_2$ are crucial to the relative sizes of the back scattering and forward scattering, since cases $d_1 < d_2$, $d_1 \simeq d_2$ or $d_1 > d_2$ will give different results.

### *3.2. The scattering cross section*

The differential cross section is given by (Nkoma and Loudon 1975)

$$\frac{\mathrm{d}\sigma}{\mathrm{d}\Omega} = \frac{\varepsilon_\alpha \omega_1 A}{4\pi^2 c^2 |\boldsymbol{E}^{1}_{1}|^2} \sum_{q\beta z} \omega_s \cos^2\theta_{\alpha s} |\boldsymbol{E}^{s}_{\alpha}|^2 \tag{46}$$

where $\alpha = 1$ and 4 for back and forward scattering, respectively, and $A$ is the area on the surface where the beam emerges. To proceed, we make the following approximations for the scattered fields given in (33) and (43). Recall that from equations (44) and (45), we have

$$K_{2z} + k^{s}_{2z} \gg K_{2z} - k^{s}_{2z}. \tag{47}$$

Therefore, all terms with $K_{2z} + k^{s}_{2z}$ in their denominators can be considered to be negligible as discussed towards the end of § 3.1 and in the references cited there. Using this fact, and equations (33)–(43) in (46), we obtain the back-scattering cross section as

$$\left(\frac{\mathrm{d}^2\sigma}{\mathrm{d}\Omega\,\mathrm{d}\omega_s}\right)_B = \frac{\hbar\varepsilon_1\omega_1\omega_s^3}{4\pi^3\varepsilon_0^2 c^4}\cos^2\theta_{1s}\,[n(\omega)+1]\hat{\boldsymbol{e}}^{1}_{i'}\cdot\hat{\boldsymbol{e}}^{1}_{i}$$
$$\times \sum_f \left[\left|\frac{1}{\Delta_f}\left(\frac{B^{-}_{2fh}f_{21}C_{2hij}}{k^{1}_{2z} - k^{s}_{2z} - q_{2z}} + \frac{B_{3fh}f_{31}C_{3hij}\mathbf{R}_{32}}{k^{1}_{3z} - k^{s}_{3z} - \tilde{q}_{3z}}\right)\right|^2\right.$$

$$+\left|\frac{1}{\Delta_f}\left(\frac{B^{+}_{2fh}f_{21}C_{2hij}}{k^{l}_{2z}-k^{s}_{2z}+q_{2z}}+\frac{B_{3fh}f_{31}C_{3hij}\mathbf{R}_{32}}{k^{l}_{3z}-k^{s}_{3z}+q_{3z}}\right)\right|^{2}\Bigg)$$
$$\times \operatorname{Im}(\langle\langle E_{0x};E_{0x}\rangle\rangle+\langle\langle E_{0z};E_{0z}\rangle\rangle) \tag{48}$$

where

$$B^{\pm}_{2fh}=\exp[-\mathrm{i}(k^{s}_{1z}d_1+k^{s}_{3z}d_2]\{\varphi_{2f}g^{+}_{fh12}\exp[\mathrm{i}(k^{l}_{2z}+k^{s}_{2z}\pm q_{2z})d_1]$$
$$+\varphi_{4f}g^{-}_{fh12}\exp[\mathrm{i}(k^{l}_{2z}-k^{s}_{2z}\pm q_{2z})d_1]-\varphi_{2f}g^{-}_{fh23}\zeta_{fh}-\varphi_{4f}g^{+}_{fh23}\zeta_{fh}\} \tag{49}$$

$$B_{3fh}=\exp[-\mathrm{i}(k^{s}_{1z}d_1+k^{s}_{3z}d_2)](\varphi_{2f}g^{-}_{fh23}+\varphi_{4f}g^{+}_{fh23}) \tag{50}$$

$$C_{2hij}=a^{\nu}_{2hij}\beta^{\nu}_{2j}+b_{2hij} \tag{51}$$

$$C_{3hij}=a^{\nu}_{3hij}\beta^{\nu}_{3j}+b_{3hij} \tag{52}$$

and $\hat{\boldsymbol{e}}^{l}_{i}$, $\hat{\boldsymbol{e}}^{l}_{i'}$ are unit polarisation vectors of the incident light in region I. The superscripts $\pm$ in (49) refer to the corresponding sign of $\pm q_{2z}$ on the right-hand side of that equation, and all other symbols are as defined earlier. Following a similar procedure as above, the forward-scattering cross section is obtained as

$$\left(\frac{\mathrm{d}^2\sigma}{\mathrm{d}\Omega\,\mathrm{d}\omega_s}\right)_{\mathrm{F}}=\frac{\hbar\varepsilon_4\omega_1\omega_s^3A}{4\pi^3\varepsilon_0^2c^4}\cos^2\theta_{4s}\,[n(\omega)+1]\hat{\boldsymbol{e}}^{l}_{i}\cdot\hat{\boldsymbol{e}}^{l}_{i'}$$
$$\times\sum_f\Bigg[\left|\frac{1}{\Delta_f}\left(\frac{F^{-}_{2fh}f_{21}C_{2hij}}{k^{l}_{2z}-k^{s}_{2z}-q_{2z}}+\frac{F^{-}_{3fh}C_{3hij}\mathbf{R}_{32}}{k^{l}_{3z}-k^{s}_{3z}-q_{3z}}\right)\right|^{2}$$
$$+\left|\frac{1}{\Delta_f}\left(\frac{F^{+}_{2fh}f_{21}C_{2hij}}{k^{l}_{2z}-k^{s}_{2z}+q_{2z}}+\frac{F^{+}_{3fh}f_{31}C_{3hij}\mathbf{R}_{32}}{k^{l}_{3z}-k^{s}_{3z}+q_{3z}}\right)\right|^{2}\Bigg]$$
$$\times\operatorname{Im}(\langle\langle E_{0x};E_{0x}\rangle\rangle+\langle\langle E_{0z};E_{0z}\rangle\rangle) \tag{53}$$

where

$$F^{\pm}_{2fh}=\exp[\mathrm{i}(k^{s}_{4z}d_2+k^{s}_{2z}d_1)]\,[(\varphi_{3f}g^{-}_{fh23}+\varphi_{4f}g^{+}_{fh23})$$
$$+[2\varepsilon_2(\omega_s)/k^{s}_{2z}]\exp[\mathrm{i}(k^{l}_{2z}-k^{s}_{2z}\pm q_{2z})d_1]g^{-}_{fh12}(\varphi_{3f}g^{-}_{fh23}+\varphi_{4f}g^{+}_{fh23})] \tag{54}$$

and

$$F^{\pm}_{3fh}=\exp[\mathrm{i}(k^{s}_{4z}d_2+k^{s}_{2z}d_1)]\,[\{\varphi_{3f}g^{+}_{fh34}\exp[-\mathrm{i}(k^{l}_{3z}+k^{s}_{3z}\pm q_{3z})d_2]$$
$$+\varphi_{4f}g^{-}_{fh34}\exp[-\mathrm{i}(k^{l}_{3z}-k^{s}_{3z}\pm q_{3z}d_2)]-\varphi_{3f}g^{-}_{fh23}-\varphi_{4f}g^{+}_{fh23}\}] \tag{55}$$

and the superscripts $^{\pm}$ refer to the corresponding sign of $\pm q_{2z}$ and $\pm q_{3z}$ on the right hand side of (54) and (55). It will be of practical interest to find out which is the larger of the back-scattering cross section given in (48) and the forward-scattering cross section given in (53). This question will be examined in the next section. However, as expected, both cross sections depend on the imaginary part of the *xx* and *zz* response functions discussed in § 2.

## 4. Numerical results and discussion

In this section we present numerical results by using parameters for the FMS modelling a sapphire substrate–GaP–GaAs bilayer–vacuum system. Suppose that regions II and

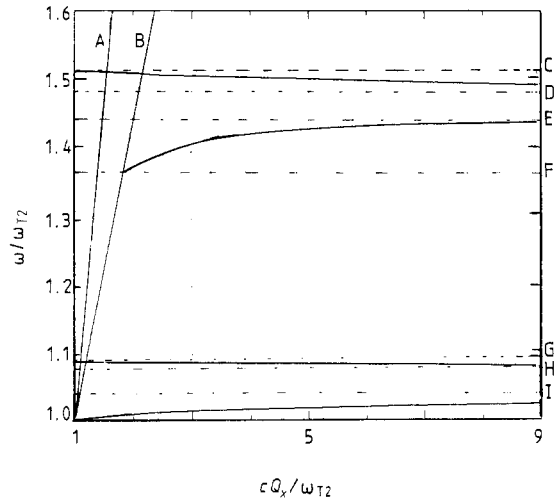


**Figure 3.** Dispersion curves for a sapphire substrate–GaP–GaAs bilayer–vacuum. The labelled frequencies—A, $\omega = cQ_x/\varepsilon_1^{1/2}$; B, $\omega = cQ_x/\varepsilon_4^{1/2}$; C, $\omega_{L3}/\omega_{T2}$; D, $\omega_{s34}/\omega_{T2}$; E, $\omega_{s23}^{+}/\omega_{T2}$; F, $\omega_{T3}/\omega_{T2}$; G, $\omega_{L2}/\omega_{T2}$; H, $-\omega_{s12}/\omega_{T2}$; I, $\omega_{s23}^{-}/\omega_{T2}$—are defined in the text.

III making the bilayer are occupied by materials whose dielectric functions are of the form

$$\varepsilon_\beta(\omega) = \varepsilon_\beta(\infty) + S_\beta\omega_{T\beta}^2/(\omega_{T\beta}^2 - \omega^2) \tag{56}$$

where $\varepsilon_\beta(\infty)$ is the high-frequency dielectric function, $S_\beta$ measures the strength of the resonance and $\omega_{T\beta}$ is the phonon frequency. The following parameters are used: the sapphire dielectric constant $\varepsilon_4$ is taken at 3.1 (Prieur and Ushioda 1975); GaP values are taken from Barker (1968) as $\varepsilon_3(\infty) = 9.09$, $S_3 = 2.01$ and $\omega_{T3} = 366.0\ \text{cm}^{-1}$; GaAs values are from Blakemore (1982) as $\varepsilon_2(\infty) = 10.88$, $S_2 = 1.97$ and $\omega_{T2} = 267.5\ \text{cm}^{-1}$. Medium I is taken as vacuum with $\varepsilon_1 = 1.0$. The thicknesses are taken as $d_1 = 3000$ Å and $d_2 = 6000$ Å and these are easily variable parameters both theoretically and experimentally. The dispersion curves from equation (21) are shown in figure 3 in terms of the reduced frequency against the reduced tangential wavevector. It can be seen that there are four branches of SPS which have four asymptotic limiting frequencies in the limit of large tangential wavevectors ($Q_x \to \infty$), and these frequencies can explicitly be given as $\omega_{s12}$, $\omega_{s23}^{+}$, $\omega_{s23}^{-}$ and $\omega_{s34}$:

$$\omega_{s12} = \{[\varepsilon_2(\infty) + S_2 + \varepsilon_1]/[\varepsilon_2(\infty) + \varepsilon_1]\}^{1/2}\omega_{T2} \tag{57}$$

$$\omega_{s34} = \{[\varepsilon_3(\infty) + S_3 + \varepsilon_4]/[\varepsilon_3(\infty) + \varepsilon_4]\}^{1/2}\omega_{T2} \tag{58}$$

$$(\omega_{s23}^{\pm})^2 = \{(f_2\omega_{T2}^2 + f_1\omega_{T3}^2) \pm [(f_2\omega_{T2}^2 + f_1\omega_{T3}^2)^2 - 4f_3f_4\omega_{T2}^2\omega_{T3}^2]^{1/2}\}/2f_3 \tag{59}$$

where

$$f_1 = \varepsilon_2(\infty) + \varepsilon_3(\infty) + S_3 \tag{60}$$

$$f_2 = \varepsilon_2(\infty) + \varepsilon_3(\infty) + S_2 \tag{61}$$

$$f_3 = \varepsilon_2(\infty) + \varepsilon_3(\infty) \tag{62}$$

$$f_4 = \varepsilon_2(\infty) + \varepsilon_3(\infty) + S_2 + S_3. \tag{63}$$

Thus the four SP branches exist in clearly defined frequency ranges, in regions where the dielectric function is negative:

$$\text{branch 1} \qquad \omega_{s34} \leqslant \omega < \omega_{L3} \tag{64}$$

$$\text{branch 2} \qquad \omega_{T3} \leqslant \omega \leqslant \omega_{s23}^{+} \tag{65}$$

$$\text{branch 3} \qquad \omega_{s12} \leqslant \omega < \omega_{L2} \tag{66}$$

$$\text{branch 4} \qquad \omega_{T2} \leqslant \omega \leqslant \omega_{s23}^{-} \tag{67}$$

where

$$\omega_{L2} = \{[\varepsilon_2(\infty) + S_2]/\varepsilon_2(\infty)\}^{1/2}\omega_{T2} \tag{68}$$

$$\omega_{L3} = \{[\varepsilon_3(\infty) + S_3]/\varepsilon_3(\infty)\}^{1/2}\omega_{T3}. \tag{69}$$

The meaning of the asymptotic frequencies is clear; $\omega_{L2}$ and $\omega_{L3}$ are the LO phonon frequencies associated with regions II and III, respectively, while $\omega_{s23}^{\pm}$ gives the frequencies associated with the GaP–GaS interface when $d_1 \to \infty$ and $d_2 \to \infty$; $\omega_{s12}$ and $\omega_{s34}$ are surface phonon frequencies for regions I–II and III–IV interfaces, respectively. With the parameters used in this paper, we find that $\omega_{L3} = 1.51\omega_{T2}$, $\omega_{s34} = 1.48\omega_{T2}$, $\omega_{s23}^{+} = 1.44\omega_{T2}$, $\omega_{T3} = 1.37\omega_{T2}$, $\omega_{L2} = 1.09\omega_{T2}$, $\omega_{s12} = 1.08\omega_{T2}$ and $\omega_{s23}^{-} = 1.04\omega_{T2}$ in decreasing order as illustrated in figure 3. Also shown in figure 3 are photon lines with equations

$$\omega = cQ_x/\varepsilon_1^{1/2} \tag{70}$$

and

$$\omega = cQ_x/\varepsilon_4^{1/2}. \tag{71}$$

To discuss light scattering, we introduce damping by adding a term with $-i\omega\gamma$ in the denominator of the dielectric function given in equation (56) and we take $\gamma = 0.005\omega_{T\beta}$. The scattering cross section has a complex frequency dependence, including the dependence on the imaginary parts of the response functions. We illustrate in figure 4 the frequency dependence of the last part of equations (48) and (53) in the form

$$|\mathrm{Im}(g_{xx})| + |\mathrm{Im}(g_{zz})| = (|\mathrm{Im}\langle\langle E_{0x}; E_{0x}\rangle\rangle| + |\mathrm{Im}\langle\langle E_{0z}; E_{0z}\rangle\rangle|)10^{-23} \tag{72}$$

for thicknesses $d_1 < d_2$ using the values mentioned earlier, where the $y$-axis values have been obtained by dividing the response functions by $10^{23}$ as shown in equation (72). It should be noted that the back and forward scattering mainly differ in the terms in the large brackets just after the summation sign in equations (48) and (53). The way that the curves in figure 4 have been plotted is as follows. It is known that for any scattering angle the response functions will peak at a certain value (or values) of frequency corresponding to a certain value of the tangential component of the wavevector $Q_x$. Hence we have plotted equation (72) for four values of the reduced wavevector $cQ_x/\omega_{T2} = 4.0, 6.0, 8.0$ and 10.0. The spectrum shows well defined peaks plus some interference effects due to the multiple boundaries. The case when $d_1 > d_2$ ($d_1 = 6000$ Å and $d_2 = 3000$ Å) is illustrated in figure 5 for similar values of the wavenumbers as earlier. The overall observable spectrum must of course include the effects of the terms in the large brackets immediately after the summation sign in equations (48) and (53), and these have not been included in figures 4 and 5. The sizes of the back- and forward-scattering cross sections will depend on how the magnitudes of terms in $B_{2fh}^{\pm}$ in (49) and $B_{3fh}$ in (50)

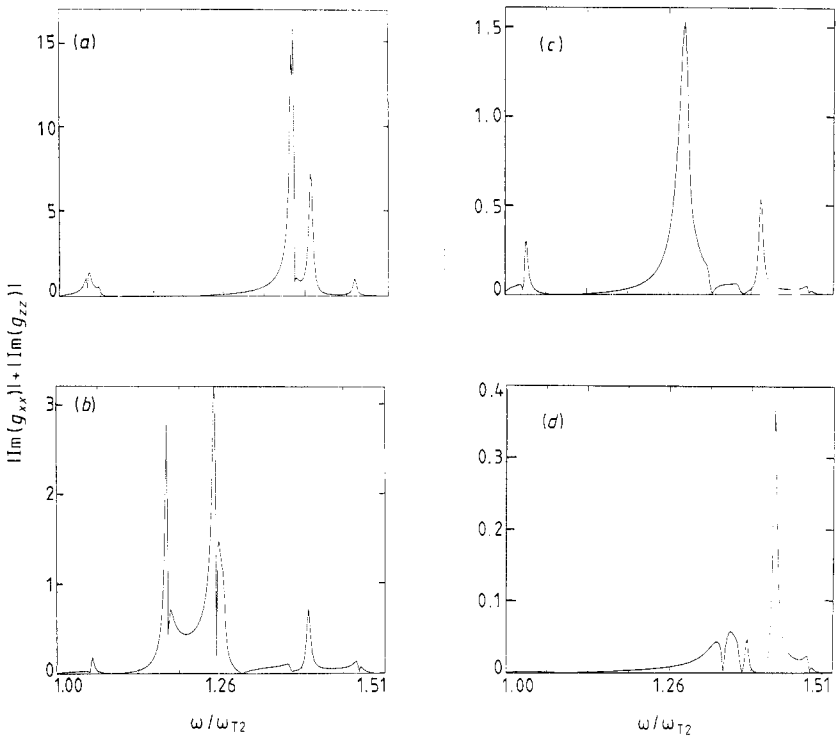


**Figure 4.** (*a*) Frequency spectrum of $|\mathrm{Im}(g_{xx})| + |\mathrm{Im}(g_{zz})|$ for (*a*) $cQ_x/\omega_{T2} = 4.0$, (*b*) $cQ_x/\omega_{T2} = 6.0$, (*c*) $cQ_x/\omega_{T2} = 8.0$ and (*d*) $cQ_x/\omega_{T2} = 10.0$; $d_1 < d_2$ ($d_1 = 3000$ Å and $d_2 = 6000$ Å).

compare with $F^{\pm}_{\tilde{2}fh}$ and $F^{\pm}_{\tilde{3}fh}$ in (54) and (55), respectively. These terms have a strong frequency dependence and size dependence as shown explicitly in their expressions.

## 5. Conclusions

In this paper, we have used the method of linear response theory in § 2 to obtain the response functions for SPs in a FMS and these have been given in equation (4). The pole of the derived response function generates the dispersion relation given in equation (21), and the dispersion curves plotted in figure 3 show that the FMS supports four branches of SPs in clearly defined frequency ranges given in equations (64)–(67) in § 4. We have presented the theory for Raman scattering by SPs in a FMS in § 3, and expressions for electric fields in the incidence plane and scattering plane have been given. By making reasonable approximations, expressions for the back- and forward-scattering cross sections have been obtained in equations (64) and (67), respectively. Both of these cross sections depend on the imaginary part of the response functions, whose spectra have been illustrated in figures 4 and 5.

We wish to conclude with the remark that, in addition to ATR experiments mentioned in the § 1, Raman scattering can also be used to study SPs in a FMS configuration. The understanding of this geometry is important since it contains the bilayer which is a basic unit in binary superlattices, which are currently receiving much attention.

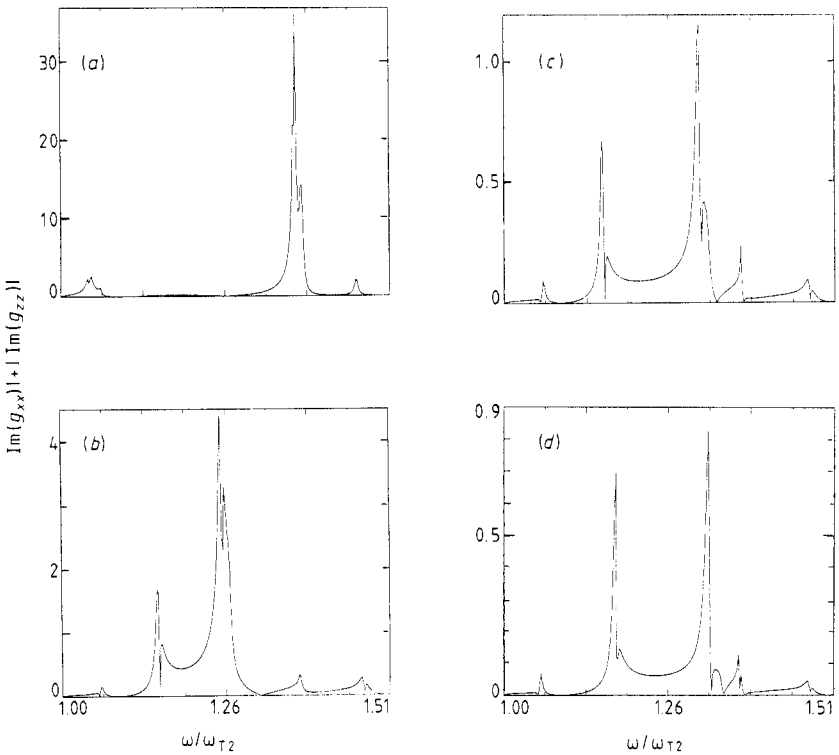


**Figure 5.** (*a*) Frequency spectrum of $|\mathrm{Im}(g_{xx})| + |\mathrm{Im}(g_{zz})|$ for (*a*) $cQ_x/\omega_{T2} = 4.0$, (*b*) $cQ_x/\omega_{T2} = 6.0$, (*c*) $cQ_x/\omega_{T2} = 8.0$ and (*d*) $cQ_x/\omega_{T2} = 10.0$; $d_1 > d_2$ ($d_1 = 6000$ Å and $d_2 = 3000$ Å).

## Acknowledgments

I would like to acknowledge hospitality at the International Centre for Theoretical Physics, Trieste, Italy, where some of this work was done.

## References

Babiker M, Constantinou N C and Cottam M G 1987a *J. Phys. C: Solid State Phys.* **20** 4581–96
—— 1987b *J. Phys. C: Solid State Phys.* **20** 4597–4612
Barker A S Jr 1968 *Phys. Rev.* **165** 917–22
Barker A S Jr and Loudon R 1972 *Rev. Mod. Phys.* **44** 18–47
Blakemore J S 1982 *J. Appl. Phys.* **53** 123–81
Boardman A D 1982 *Electromagnetic Surface Modes* (New York: Wiley)
Camley R E and Mills D L 1984 *Phys. Rev.* B **29** 1695–706
Chen Y J, Burstein E and Mills D L 1975 *Phys. Rev. Lett.* **34** 1516–9
Cottam M G and Maradudin A A 1984 *Surface Excitations* eds V M Agranovich and R Loudon (Amsterdam: North-Holland) pp 1–194
Haupt R and Wendler L 1987 *Phys. Status. Solidi* b **142** 125–39
Landau L D and Liftshitz E M 1969 *Statistical Physics* (Oxford: Pergamon)
Maradudin A A and Mills D L 1975 *Phys. Rev.* **11** 1392–415
Mills D L and Burstein E 1974 *Rep. Prog. Phys.* **37** 817–926
Mills D L, Chen Y J and Burstein E 1976 *Phys. Rev.* B **13** 4419–38

Mills D L, Maradudin A A and Burstein E 1970 *Ann. Phys., NY* **56** 504–55
Mirlin D 1982 *Surface Polaritons* ed. V M Agranovich and D L Mills (Asterdam: North-Holland) pp 3–67
Nkoma J S 1975 *J. Phys. C: Solid State Phys.* **8** 3919–36
—— 1987a *Solid State Commun.* **64** 1383–6
—— 1987b *Phys. Status Solidi* b **139** 117–23
—— 1987c *Surf. Sci.* **191** 595–607
Nkoma J S and Loudon R 1975 *J. Phys. C: Solid State Phys.* **8** 1950–68
Otto A 1968 *Z. Phys.* **216** 398–410
Prieur and Ushioda S 1975 *Phys. Rev. Lett.* **34** 1012–5
Raj N, Camley R E and Tilley D R 1987 *J. Phys. C: Solid State Phys.* **20** 5203–16
Szenics R, Wallis R F, Giuliani G F and Quinn J J 1986 *Surf. Sci.* **16** 645–56
Ushioda S 1981 *Prog. Opt.* **19** 139–210
Ushioda S and Loudon R 1982 *Surface Polaritons* ed. V M Agranovich and D L Mills (Amsterdam: North-Holland) pp 535–86
Wendler L 1984 *Phys. Status Solidi* b **123** 469–77
—— 1985 *Phys. Status Solidi* b **128** 425–37
Wendler L and Haupt R 1986 *Phys. Status Solidi* b **137** 269–90
—— 1987 *Phys. Status Solidi* b **143** 131–48